# Dynamic Light Scattering Study of Nematic and Smectic-*A* Liquid Crystal Ordering in Silica Aerogel

Tommaso Bellini,[1,2] Noel A. Clark,[2] and Dale W. Schaefer[3]
[1]*Dipartimento di Elettronic, Universita' di Pavia 27100 Pavia, Italy*
[2]*Condensed Matter Laboratory, Department of Physics, University of Colorado, Boulder, Colorado 80309*
[3]*Sandia National Laboratories, Albuquerque, New Mexico 87185*
(Received 25 April 1994)

The dynamical behavior of nematic and smectic-*A* ordering of a liquid crystal in an aerogel host is studied by quasielastic light scattering. In the nematic phase, ordered domains are comparable to the pore size and generally frozen in orientation, with remnant orientation fluctuations having paranematic dynamics for a domain size distribution appropriate to the aerogel, and the coupling between domains giving rise to an additional slow glasslike relaxation. At lower temperatures a drastic slowing down, connected with a local nematic–to–smectic-*A* transformation, is observed.

PACS numbers: 64.70.Md, 61.30.Eb, 78.35.+c, 82.70.Gg

The study of the phase behavior of liquid crystals in porous media offers experimental access to the effects of externally induced disorder on a wide variety of phase transitions [1,2]. This Letter concerns the dynamics of the ordering processes of the isotropic, nematic, and smectic-*A* phases of the liquid crystal 8CB incorporated into silica aerogel. It has been established using static light scattering and calorimetry that 8CB in a 200 Å mean pore-size aerogel has local nematiclike orientational ordering [1], and x-ray diffraction has exhibited the smectic-*A*-like one-dimensional fluid layer translational ordering [2] within the nematic domains. Here we probe the evolution of the dynamics of these ordering events using quasielastic light scattering (QELS) from molecular orientation fluctuations, finding evidence for a novel sequence of three distinct dynamic processes. Recently Wu *et al.* used QELS to study the nematic ordering of 8CB in sintered porous silica [3], finding orientational glasslike dynamics near the nematic-isotropic transition. This behavior will be compared to the following rather different scenario found in the aerogels.

(1) *Nematic intrapore orientation fluctuations.*—On the intrapore length scale, in all the nematic range, there is a distinctive bimodal behavior with the liquid crystal orientation fluctuations frozen out in the smallest pores. Fluctuations in larger pores give orientation correlation functions obtainable from the orientational dynamics of paranematic fluctuations in domains having the size distribution of the pores in the aerogel.

(2) *Nematic pore-pore orientational coupling.*—A slow relaxation, diverging in decay time and becoming nonergodic as temperature is lowered, dominates the tail of the orientational correlation function (OCF), suggesting that the orientational field resembles a spin system undergoing a spin-glass transition on an interpore length scale larger than the nematic domain size.

(3) *Smectic slowing down.*—Upon lowering the temperature into the smectic-*A* phase, a dramatic slowing of the intrapore orientational dynamics marks the growth of smectic clusters inside the nematic domains. The dynamic scaling of the OCF suggests an energy landscape with increasing barrier heights for nematic defect motion as the smectic order develops.

QELS was carried out on 8CB-aerogel systems of three different aerogel densities, for temperatures ranging from the isotropic phase to well below the bulk nematic–smectic-*A* transition. Bulk 8CB exhibits isotropic (*I*), nematic (*N*), smectic-*A* (*A*), and crystal (*X*) phases vs temperature $T$ as follows [4–6]: $I$ ($T_{IN}$ = 40.5 °C) $N$ ($T_{NA}$ = 33.7 °C) $A$ ($T_{AX}$ = 21.5 °C) $X$. The aerogels used here [7] have mass densities $\rho$ = 0.60, 0.36, and 0.08 g/cc; mean solid chord lengths of ~58, 45, and 43 Å; pore sizes (pore chord lengths) of $\xi_p$ = 98, 175, and 600 Å; and pore volume fractions of $\phi$ = 0.63, 0.79, and 0.94, respectively. The 8CB-aerogel samples were prepared under vacuum using capillary action in the nematic phase to fill 1 mm thick slabs of aerogel. Residual liquid crystal on the surfaces was removed in the isotropic phase. The QELS was carried out using a 6328 Å He-Ne laser and a Brookhaven 9000 correlator operating over delay times in the range 1 $\mu$s $\leq t \leq$ 10 s. Scattered light was collected at a scattering angle $\theta$ = 60°. There was no significant dependence of the QELS time correlation functions on polarization or $\theta$.

In Fig. 1 we show a typical family of heterodyne correlation functions $g_1(t)$ obtained over the range 18 < $T$ < 40.5 °C in the 0.36 g/cc aerogel. This evolution is qualitatively similar in the other aerogels. The family exhibits the following scenario as $T$ is decreased. As $T$ is lowered through $T_{NI}$ (dashed curves), the decay comes into the time range of the correlator and by $T = T_{NI} - 0.5$ °C evolves to a fast relaxation which is completed in ~100 $\mu$s. As $T$ is further lowered in the nematic range, there develops an increasingly slow second relaxation (solid curves), which ultimately exceeds the long time range of the correlator, giving an almost

 0031-9007/95/74(14)/2740(4)$06.00 

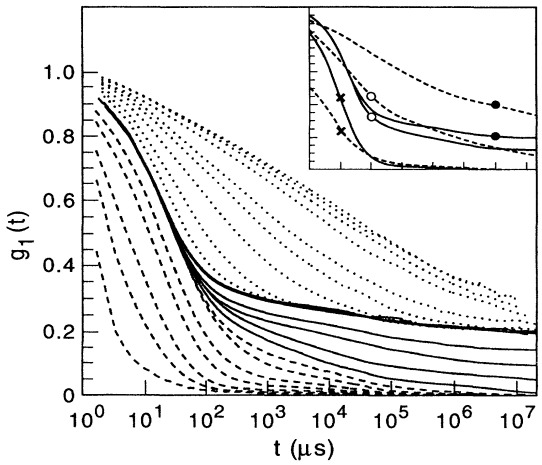


FIG. 1. Evolution of $g_1(t)$ for the 8CB 0.36 g/cc aerogel sample vs temperature. The three different regimes discussed in the text are identified by different kinds of lines: (---), intrapore "fast nematic" relaxation regime ($T$ = 40.32 °C, 40.21 °C, 40.11 °C, 39.89 °C, 39.71 °C, 39.48 °C, and 39.11 °C); (—), interpore "nematic glass" transition regime ($T$ = 38.8 °C, 38.69 °C, 38.31 °C, 37.58 °C, 35.42 °C, 34.45 °C, and 32.96 °C); (···), intrapore "smectic slowing down" regime ($T$ = 30.96 °C, 29.01 °C, 27.01 °C, 25.04 °C, 23.55 °C, 22.09 °C, 21.11 °C, 20.13 °C, and 18.19 °C). Inset: overplot of $g_1(t)$ from Ref. [3] (---) for 8CB in sintered porous glass and from our aerogel data (—) at $T$ = 40 °C (x), 38 °C (○), and °C (•) (axes labels same as for main plot).

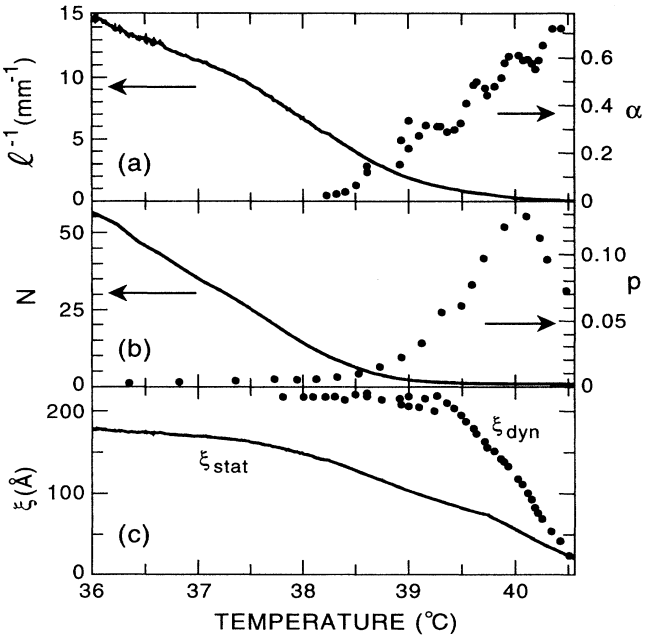


FIG. 2. Data vs $T$ for the 0.36 g/cc aerogel: (a) (—) $\ell^{-1}$, inverse optical mean free path (from Ref. [1]), and (•) $\alpha$, the exponent of stretched exponential slow relaxation. (b) (•) $p$, probability that a scattering event comes from a dynamically fluctuating site, and (—) $N$, the average number of scattering events per path. (c) (•) $\xi_{dyn}$, mean nematic domain size obtained from the fast intrapore nematic relaxation, and (—) $\xi_{stat}$, nematic domain size obtained form $\ell^{-1}$ (from Ref. [1]).

constant background at large $t$. For $32 < T < 36$ °C, the combined relaxation curves become independent of $T$. Then, for $T < 32$ °C, the fast relaxation begins to dramatically slow. These processes will now be discussed separately.

Figures 2(a) and 2(c) show, respectively, the inverse mean free path $\ell^{-1}$ and orientational correlation length $\xi_{stat}$ of the 8CB 0.36 g/cc system, previously obtained via static light scattering measurements and a model of scattering by a polydomain nematic [1]. Because the mean free path $\ell$ becomes small compared to the sample thickness $d$ = 1 mm, at low $T$, the $g_1(t)$ are taken in the multiple scattering regime, with an increasing number $N(T)$ of scattering events per diffusive optical path as $T$ is lowered, as shown in Fig. 2(b) [8]. However, decreasing $\ell$ did not produce the faster relaxation of $g_1(t)$ expected for multiple scattering [9]. Also the contrast of the ensemble averaged correlation function $C = [g_1(0) - g_1(\infty)/g_1(\infty)$ decreased. This observation led us to calculate the probability $p$ that a scattering event comes from a dynamically fluctuating site, which can be evaluated from $C(T)$ and $N(T)$. The resulting $p(T)$ is shown in Fig. 2(b). Since $p$ is small the scattering is mostly static with $n(T) = N(T)p(T)$ the number of dynamic scattering events per path, much less than 1, in the range $0.05 < n(T) < 0.15$ for all $T$. More importantly, the great majority of the photon paths having dynamic scattering events, have *only one* dynamic scattering event [10]. This enables a single scattering interpretation of the QELS correlation functions.

*Intrapore fluctuations.*—We now analyze the fast relaxation process in terms of paranematiclike fluctuations, extracting a mean dynamic domain size $\xi_{dyn}$. The fast relaxation is nonexponential, indicating a process with a broad distribution of relaxation times. This behavior can be obtained using the polydomain nematic model of Ref. [1], assuming that the orientation fluctuations of each domain (dimension $L$) contribute a single exponential relaxation whose decay time is, as in the bulk, proportional to $L^2$ [11]. Using a domain size distribution obtained from the observed [2] void-void correlation function of the empty aerogel, $P(L) \propto [e^{-L/\xi_{dyn}}]L^{-2}$, where $\xi_{dyn}$ is the mean domain size, we can write the appropriate superposition integral $R_F(t/t)$ for the heterodyne scattered light field correlation function of the fast relaxation

$$R_F(t') = A_F \xi_{dyn}^5 \int_0^\infty [\exp(-y)y^{-2}]\exp(t'/y^2)y^6\, dy\,, \qquad (1)$$

where $t' = t/D\xi_{dyn}^2$, and $A_F$ is the amplitude. The orientational diffusivity $D$ can be obtained from the exponential pretransitional bulk relaxation as $D = \tau_{NI}/[x_{NI}]^2$, where $\tau_{NI}$ = 0.4 μs and $\xi_{NI}$ = 85 Å are the isotropic relaxation time and correlation length at $T_{NI}$, respectively [11,12]. The fit involves three parameters $\xi_{dyn}$, the baseline, and $A_F$. For $T$ in the range $32.5 < T < 40$ °C, the

fits are quite good, indicating that the *shape* of $g_1(t)$ is $T$ independent and that the model matches the relaxation time distribution of Eq. (1) well. Figure 3 shows a typical fit of Eq. (1) [dashed curve] to $g_1(t)$ in the interval 1 $\mu$s $< t <$ 30 $\mu$s for $T = 39.5$ °C. For $T > 40$ °C, the shape of $g_1(t)$ is not invariant vs $T$, developing into a bimodal fast initial decay and distinct tail. This is the $T$ range where, as $T$ decreases, the nematic is most rapidly growing in the pores and the bimodal decay is probably due to the growth of the nematic ordering first in the large pores, i.e., a suppression of nematic order in the small pores. Given $D$, for $T < 40$ °C, where Eq. (1) fits the measured $g_1(t)$, we can calculate $\xi_{\rm dyn}$ from the fitted values of $\tau_F$, with the result shown in Fig. 2(c). For $T > 40$ °C, an effective $\tau_F$ was obtained from $T_1 = \int_0^\infty g_1(t)\,dt$, the first moment of $g_1(t)$, as $\tau_F = \gamma T_1$ with $\gamma = \frac{1}{30}$, the value for the size distribution in Eq. (1). As is clearly noticeable, upon decreasing $T$, $\xi_{\rm dyn}$ grows and saturates at about $T = 39.3$ °C to a value $\xi_{\rm dyn} \sim 215$ Å, comparable to the 0.36 g/cc aerogel pore chord $\xi_p \sim 175$ Å. The same procedure leads to low-$T$ values of $\xi_{\rm dyn} = 115$ Å and $\xi_{\rm dyn} = 430$ Å for 0.6 g/cc and 0.08 g/cc aerogels, respectively, which can be compared to their respective pore chords $\xi_p \sim 100$ and 600 Å. Also shown in Fig. 2(c) is $\xi_{\rm stat}$. The different variation of $\xi_{\rm dyn}$ and $\xi_{\rm stat}$ with $T$ presumably arises from their different dependence on the pore size distribution. If, upon decreasing the temperature, the asymptotic $P(L)$ is reached through a faster filling of the larger pores by the nematic phase $\xi_{\rm stat}$, which is more sensitive than $\xi_{\rm dyn}$ to the small domain part of the distribution, should indeed grow more slowly than $\xi_{\rm dyn}$. For the same reason it is likely that the static scattering background comes from frozen smaller domains, more relevant to the turbidity than to dynamic behavior.

*Pore-pore orientational coupling.*—A qualitative inspection of the correlation functions presented in Fig. 1 shows that a slow relaxation, barely noticeable when $T > 40$ °C, grows to dominate the long time relaxation of $g_1(t)$ as $T$ is decreased (solid curves). This indicates that the fast relaxation mechanism does not completely uncorrelate the director orientation, as one would expect for uniaxial domains free to rotate. Upon lowering $T$, the order parameter and elastic constants increase, enabling domains to grow by excluding defects, to a limit imposed by the aerogel. As domain growth becomes restricted by the aerogel matrix, there is little further change in the fast relaxation dynamics; the dynamic correlation length stops growing, and the slow relaxation appears, suggesting that the slow relaxation is a result of rotational diffusion being hindered by an increasingly hilly energy landscape, which may result from coupling either to the aerogel and frozen domains (acting as a local random orientational field) or to other fluctuating domains (as in a spin system with random interactions), or both. As $T$ is lowered, the increasing coupling has the effect of saturating the faster relaxation at progressively earlier stages. The data as well as the possible analogy to a spin system undergoing a glass transition [13] suggest using the stretched exponential (SE) function $R_S(t) = A_S \exp[-(t/\tau_S)^\alpha]$ to fit the slow relaxation of $g_1(t)$. This fit was carried out, combining the fast and long time processes in such a way that the long-time process removes correlations left after the completion of the fast process. This was done, as indicated in Fig. 3, by inserting in $R_F(t)$ an exponential saturation of $t$, like that of the correlation function of intensity scattered by Brownian oscillators [14] $R_F(t) \rightarrow R_F(\delta[1 - e^{-t/\delta}])$, where $R_F(\delta)$ is the saturated value of $g_1(t)$ at the completion of the fast process. With this procedure the $g_1(t)$ curves could be fitted over their whole time range and, in particular, the slow relaxations were well fitted by stretched exponentials, as Fig. 3 indicates.

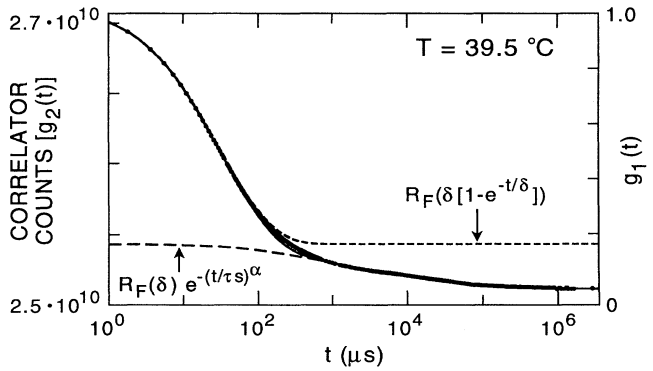


FIG. 3. (Left scale): measured QELS intensity correlation function $g_2(t)$ of unpolarized light scattered by the 0.36 g/cc aerogel at $T = 39.5$ °C and $q = 60°$ (• • •); [right scale]: The corresponding $g_1(t)$ [$g_2(t)$ baseline subtracted and normalized to an amplitude of 1]. Also shown is the fit to the composite fast-slow relaxation form $g_1(t) = R_F(\delta[1 - e^{-t/\delta}]) - R_F(\delta) + R_F(\delta)\exp[-(t/\tau_s)^\alpha]$ (—), and its constituent fast (---) and slow stretched exponential (– – –) relaxation components.

In Fig. 2(a) we show the SE exponent $\alpha$ for the 0.36 g/cc aerogel sample, which decreases from 1 to 0 as $T$ is lowered. This and the accompanying drastic increase of the slow process decay time are characteristic of spin-glass-like behavior [3,15] and support the notion that the slowing down is due to the *interpore* coupling of domains in which the director, coupled via various channel structures between pores, corresponds to spins placed on a disordered lattice with varying nearest-neighbor interactions. This glassy relaxation model, as well as the random field model for the nematic to isotropic transition [16], leads to nonergodic behavior. In a *homodyne* DLS one can check for this by moving the sample and comparing the ensemble and time averaged $g_2(t)$'s [14]. The same cannot be done in our heterodyne DLS, where the local field is given by a static speckle pattern generated by the sample itself. We determine the "true" baseline by requiring $\tau_F$ to retain its saturated value, obtained for 39.3 °C $< T <$ 38.4 °C (see Fig. 2), at lower $T$. By doing so we obtain a continuous and monotonic behavior for $\alpha$, $A_F/A_S$, and $\tau_S$, which we do not obtain if the nonergodicity hypothesis is not adopted.

Note, in Fig. 1, the perfect superposition of the $g_1(t)$ for $33 < T < 35.5\,^{\circ}\mathrm{C}$, suggesting that the $T$ dependence of the viscosity is negligible.

It is of interest to compare this nematic dynamic behavior with that found by Wu *et al.* for 8CB in a sintered porous silica (SPS) of nominally similar pore size [3]. In the inset of Fig. 1 we overplot our aerogel $g_1(t)$ with those from the SPS. The aerogel and SPS correlation functions have similar divergent slow decays leading to orientational glass behavior but the SPS do not show the fast relaxation, indicating that the angular range of fast fluctuations is smaller in the SPS than in the aerogel. This may be because the smoother pore surfaces and lower void volume fraction and connectivity of the SPS make the effective local field stronger. The spin glass interpretation given here for the aerogel and the random field interpretation given in Ref. [3] are consistent with these geometrical differences. However, it is likely that both pore-surface and pore-pore interactions are operative in both systems.

*Smectic slowing down.*—As visible in Fig. 1, for $T < 33.7\,^{\circ}\mathrm{C}$, near the bulk $T_{NA}$, there begins a drastic slowing down of the intrapore relaxation process. Such a "smectic slowing down" changes the shape of the correlation functions: They cannot be fitted at the lower temperatures with the same $R_F(t)$ used for $T > 33\,^{\circ}\mathrm{C}$. Figure 4 shows, however, that they can be made to overlap very well by stretching the $\log(t)$ axis, and the inset gives a measure of the slowing down by showing $\tau_{SA}(T)$, the time needed for $g_1(t)$ to reach the value 0.5 of the slow decay, for the three different aerogels. The nematic behavior at higher $T$ indicates that this smectic slowing down process is essentially *intrapore*, a local director fluctuation about the overall nonergodic orientation state. The $\log(t)$ scaling that we find generally appears for activated kinetics with barriers over a broad range in energy, such as in the random field or vortex glass systems [17], the slowing down being a result of a general increase in the mean barrier height [13]. The only available pore-level fluctuation mechanism of this type in the present case appears to be the thermal motion of nematic defects, e.g., disclination lines, which encounter increasing energy barriers as the smectic order develops. X-ray data [2] on the smectic layering correlation length $\xi$ lend qualitative support to this idea in that, for the 0.36 aerogel $\xi$ increases from $\xi \sim 50$ Å at $T = 33\,^{\circ}\mathrm{C}$ to saturation at the pore size $\xi \sim 200$ Å at $T = 20\,^{\circ}\mathrm{C}$ [2], exhibiting a $T$ dependence similar to the slowing down scaling time $\tau_{SA}$ shown in the inset of Fig. 4. In each of the aerogels the slowing down process saturates at a $T$ comparable to that where the $\xi$ saturates to be comparable to the pore size. This $\log(t)$ scaling of the nematic orientational relaxation in the smectic strongly resembles that of the SPS [3] in the nematic. Both can be interpreted as resulting from activated motion of disclinations, limited by pore surfaces in the SPS and be smectic ordering in the aerogel.

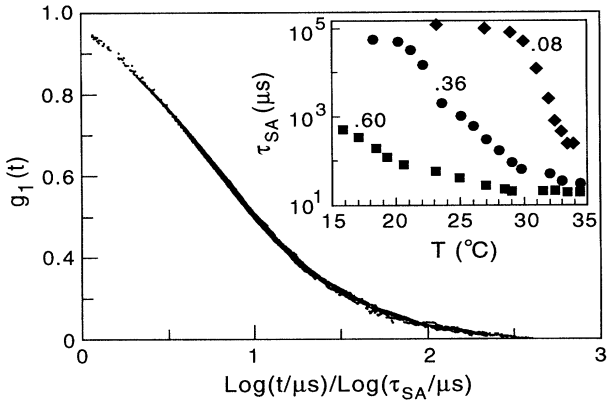


FIG. 4. Superposition of $g_1(t)$ for the 0.36 g/cc aerogel at different temperatures in the smectic slowing down regime, obtained by appropriate scaling of the various $\log(t)$ axes. The data are for $T = 18.19\,^{\circ}\mathrm{C}$, $20.13\,^{\circ}\mathrm{C}$. $21.11\,^{\circ}\mathrm{C}$, $22.09\,^{\circ}\mathrm{C}$, $23.55\,^{\circ}\mathrm{C}$, $25.04\,^{\circ}\mathrm{C}$, $26.01\,^{\circ}\mathrm{C}$, and $27.01\,^{\circ}\mathrm{C}$. Inset: the temperature dependence of the half-decay relaxation time $\tau_{SA}$ for the three different aerogel densities: 0.60 g/cc (■), 0.36 g/cc (•), and 0.08 g/cc (♦).

We acknowledge useful conversations with C. Garland, C. Muzny, P. Pusey, and M. Corti. This work was supported by NSF Solid State Chemistry Grant No. DMR 92-23729 to N. A. C. and a NATO Grant to T. B.

[1] T. Bellini *et al.*, Phys. Rev. Lett. **69**, 788 (1992).
[2] N. A. Clark *et al.*, Phys. Rev. Lett. **71**, 3505 (1993).
[3] X-l. Wu *et al.*, Phys. Rev. Lett. **69**, 470 (1992).
[4] P. P. Karat and N. V. Madhusudana, Mol. Cryst. Liq. Cryst. **36**, 51 (1976).
[5] D. Davidov *et al.*, Phys. Rev. B **19**, 1657 (1979).
[6] G. B. Kasting *et al.*, J. Phys. (Paris) **41**, 879 (1980); J. Thoen *et al.*, Phys. Rev. A **26**, 2886 (1982).
[7] D. W. Schaefer *et al.*, in *Physics and Chemistry of Porous Media—II,* edited by J. R. Banavar, J. Koplik, and K. W. Winkler, AIP Conf. Proc. No. 154 (AIP, New York, 1983), p. 63.
[8] $N \approx 1 + d/4p^2$ for all $\ell$ here.
[9] D. J. Pine *et al.*, in *Scattering and Localization of Classical Waves in Random Media,* edited by P. Sheng (World Scientific, Singapore, 1990).
[10] For $N_j$ = number of paths having $j$ dynamical events. We find $N_2/N_1 < 0.13$ for all $T$. For $N > 10$ and $p \ll 1$: $N_2/N_1 = \frac{1}{2}\ln[(2 - C)/(2 - 2C)]$.
[11] B. Pouligny *et al.*, Mol. Phys. **49**, 583 (1983).
[12] W. Chen *et al.*, Phys. Rev. Lett. **62**, 1860 (1989).
[13] K. Binder and A. P. Young, Rev. Mod. Phys. **58**, 801 (1986).
[14] P. N. Pusey and W. van Megen, Physica (Amsterdam) **157A**, 705 (1989).
[15] R. Rammal, in *Time-Dependent Effects in Disordered Materials,* edited by R. Pynn and T. Riste, NATO ASI, Ser. B, Vol. 167 (Plenum Press, New York, 1987).
[16] A. Maritan *et al.*, Phys. Rev. Lett. **72**, 4113 (1994).
[17] D. S. Fisher *et al.*, Phys. Rev. B **43**, 130 (1991).